All-Plasmonic IQ Modulator with 36 µm Fiber-to-Fiber Pitch

Author(s):
Ayata, Masafumi; Fedoryshyn, Yuriy; Heni, Wolfgang; Josten, Arne; Bäuerle, Benedikt; Haffner, Christian; Hoessbacher, Claudia; Koch, Ueli; Salamin, Yannick; Elder, Delwin L.; Dalton, Larry R.; Leuthold, Juerg

Publication date:
2018

Permanent link:
https://doi.org/10.3929/ethz-b-000316169

Originally published in:
https://doi.org/10.1109/ECOC.2018.8535525

Funding acknowledgement:
688166 - A generic CMOS-compatible platform for co-integrated plasmonics/photonics/electronics PICs towards volume manufacturing of low energy, small size and high performance photonic devices (SBFI)
670478 - Plasmonic-Silicon-Organic Hybrid – a Universal Platform for THz Communications (EC)

All-Plasmonic IQ Modulator with 36 µm Fiber-to-Fiber Pitch

M. Ayata[(1)], Y. Fedoryshyn[(1)], W. Heni[(1)], A. Josten[(1)], B. Baeuerle[(1)], C. Haffner[(1)], C. Hoessbacher[(1)], U. Koch[(1)], Y. Salamin[(1)], D. L. Elder[(2)], L. R. Dalton[(2)], J. Leuthold[(1)]

[(1)] Institute of Electromagnetic Fields (IEF), ETH Zurich 8092 Zurich, Switzerland, mayata@ethz.ch
[(2)] University of Washington, Department of Chemistry, Seattle, WA 98195-1700, USA

Abstract *An all-plasmonic IQ-modulator with a fiber-to-fiber length of 36 µm is demonstrated at line-rates up to 200 Gbit/s. All the components: Grating couplers, polarization rotators, splitters and phase shifters are based on metal.*

Introduction

In-phase and quadrature (IQ) modulators have become key elements in optical long-haul communications as they enable the encoding of quadrature amplitude modulation (QAM). QAM modulation formats are increasingly deployed in long- and medium-haul communication systems and - if the footprint were smaller and fabrication complexity would be simpler, they would likely find applications in short-haul and even data-center networks[1, 2].

IQ-modulators encode information on both real and imaginary parts of the optical carrier by utilizing two nested Mach-Zehnder modulators (MZMs). Well-established technologies rely on $LiNbO_3$, InP, or the Silicon-Organic-Hybrid (SOH) platform[3-5]. However, devices based on these technologies end up with relatively large footprints (>0.5 mm long active section).

In order to achieve both higher integration densities and higher speed, plasmonic modulators have been introduced[6-8]. For instance, Pockels-effect plasmonic modulators, that exploit the strong light-matter interaction in metal-insulator-metal (MIM) slot waveguides, have already successfully shown their performance beyond 100 Gbit/s with low driver-voltage operation of 0.7 V_{pp} and frequency responses beyond 500 GHz[9, 10]. And while the active section in these plasmonic devices has now shrunk to the microscale, the coupling sections start to dominate the footprint. Recently, we introduced a most compact all-plasmonic MZM that was comprised of a single metal layer with built-in fiber-couplers and Mach-Zehnder interferometer[8]. The question now is if more complex IQ-modulators with a higher integration density are feasible at all.

In this paper, we introduce a most compact high-speed IQ-modulator of 36 µm length. The modulator is realized as an all-plasmonic integrated circuit with metallic couplers, polarization rotators, splitters and plasmonic phase modulators. The plasmonic IQ-modulator has been tested for speeds up to 200 Gbit/s quadrature phase-shift keying (QPSK) within bit-error ratios (BERs) of 3.64×10^{-3}. The modulator is technology agnostic, i.e., the modulator does not require a particular fabrication platform such as silicon photonics because it only relies on metal and a spin-coated layer of organic electro-optic (OEO) material and therefore can be fabricated on nearly any smooth insulating surface.

Principle of operation

The all-metallic IQ-modulator consists of four components: Vertical grating couplers (GCs), polarization rotators, splitters, and phase modulators as depicted in Fig. 1. The vertical grating coupler converts the input mode of a multicore fiber (MCF: 36 µm pitch) into surface plasmon polaritons (SPPs). The laser signal can be coupled in and out through the cores of the MCF. The initial polarization of the SPPs is vertically aligned, but rotated by the polarization rotator to match the horizontal polarization of the MIM slot waveguides. Afterwards, the energy is split upon the four arms of the IQ-modulator. The MIM slots are filled with an OEO material which induces a refractive index change through the Pockels effect[11].

The electrical signals are applied to the inner I and Q contacts, S_I and S_Q, see Fig. 1(b). Since these contacts are geometrically isolated, we utilize three-dimensional bridge structures to electrically connect them with the external electrodes.

For the optimal operation of the IQ-modulator, we implement the required π/2 phase difference between I and Q MZMs by applying geometrical distortions, see Fig. 2. The upper arm (I-MZM) has a wider slot width of Δw than the lower arm (Q-MZM), and the modulator is geometrically misaligned by Δy in y direction, resulting a longer optical path for the Q-MZM. Furthermore, we design the MIM phase modulators with different slot widths for the π phase difference within both MZMs to operate them in the null point[6]. It should be noted that an IQ-modulator has an inherent 3 dB insertion loss due to the combining of the I and

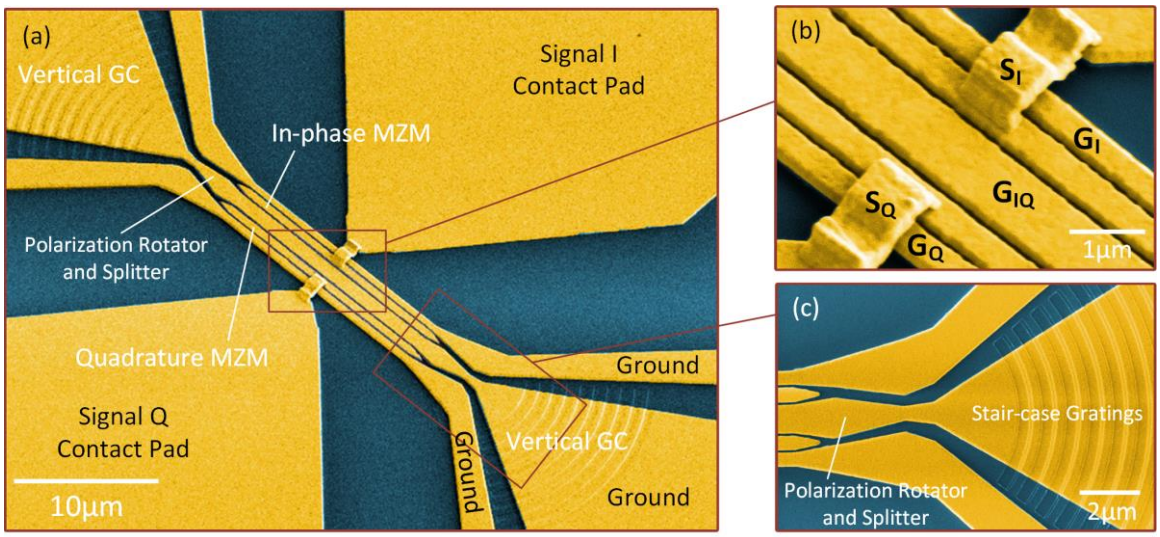

Fig. 1: False-color SEM images of the IQ-modulator. (a) Perspective view: Light is coupled via the vertical grating as surface plasmon polaritions towards the polarization rotators, where the signal's polarization is rotated, converted to gap plasmons and split onto four arms. The light is then modulated at the phase modulators and coupled out via grating coupler to another core of the MCF. (b) Magnified image of the phase modulators. The I and Q modulators share a ground contact. Signal contacts are connected to the external electrodes by suspending bridge structures. (c) Magnified image of the grating coupler, polarization rotator and splitter. The grating coupler has a stair-case grating profile to achieve uni-directional coupling

Q MZMs in a 3 dB splitter.

All the components are made of gold and lie within a distance confined to only 36 μm, matching to the core distance of the MCF.

Device fabrication

The IQ modulators were fabricated on a 6.2 μm-thick SiO_2 layer thermally grown on a silicon wafer. First, we deposited a gold layer by electron-beam evaporation (Evatec501) with a thickness of 200 nm. We used the electron-beam lithography (Vistec EBPG5200) with negative-tone resist to form the device pattern. The gold layer was then dry-etched with argon (Ar) ions (Oxford IonFab300). The stair-case gratings were made by applying two-step dry-etching process with Ar-ions. The three-dimensional bridge structures were fabricated by a lift-off process with a sacrificial layer. Lastly, we spin-coated the entire chip with the nonlinear OEO material, 75%HD-BB-OH/25%YLD124[11] which also serves as a top cladding layer. The OEO material was poled by applying the voltage between G_{IQ} and G_I (or G_Q: they are electrically connected).

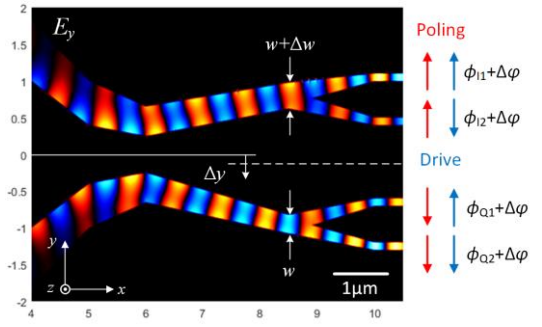

Fig. 2: Top view of electric field distribution of the E_y-field component at z = 100 nm (The gold layer has a height of 200 nm). From simulation using the finite difference time domain (FDTD) method, phase differences of ~0.5π between the I and Q MZMs can be obtained varying the access waveguide widths by Δw = 100 nm offsetting the waveguides by Δy = 100 nm. Driving voltages are applied to the inner contacts, inducing positive and negative phase shifts to each MZM.

Data experiments

The devices were tested in a coherent data transmission system setup as depicted in Fig. 3. Electrical signals were generated for I and Q modulators from a digital-to-analog converter (DAC, Micram DAC4, sampling rate: 100 GSa/s). The generated signal had the non-return-to-zero (NRZ) shape with symbol rates of 25, 50 and 100 GBd. The signals were transmitted to external electrodes of the device through GSG probes and the peak voltage after amplification was measured as V_p = 2.5 V. A continuous wave (CW) laser at 1550 nm with an output power of 14 dBm was fed into the device by means of the input-core of the MCF. The modulated signal was then coupled out to a neighbouring core from the output grating coupler of the IQ-modulator. The modulated optical signal was first amplified by a low-noise featured erbium-doped fiber amplifier (EDFA) and then filtered by an optical bandpass filter. Subsequently, the signal was fed to a coherent receiver comprised of an optical 90° hybrid and balanced photo detectors (BPDs). As a local oscillator, we split off a fraction of the input signal. Finally, the signal was digitized by a real-time oscilloscope (Sampling rate: 160 GSa/s, 3dB bandwidth: 63 GHz). The recoded

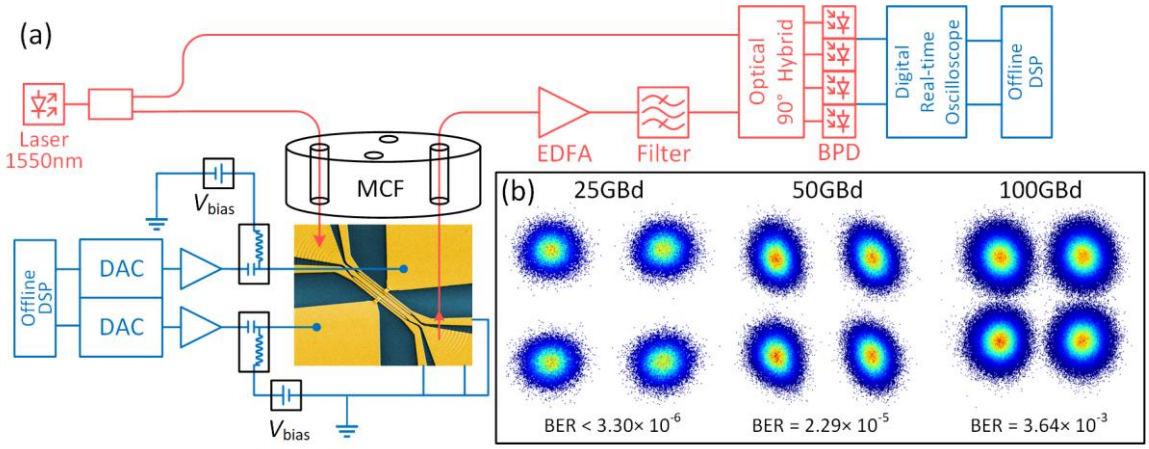

Fig. 3: Schematic of the high-speed coherent data transmission experiment. The device was tested in a homodyne detection setup. The electrical signals are generated from a DAC and we control the bias voltages of the signals to adjust the operating points of the modulator. A CW is split and one part is fed to the device and encoded with information while the other part is used for the local oscillator in the coherent receiver. The received signal is offline processed. (b) Constellation diagrams of received signals of QPSK with 25, 50 and 100 GBd (with input optical power of 8, 10 and 14dBm, respectivly). All the BERs are below the hard-decision FEC limit.

waveforms were analysed through offline digital signal processing (DSP) using Matlab. The offline DSP included static equalization, timing recovery[12], carrier phase recovery, adaptive linear and nonlinear equalization, and symbol decision.

The constellation diagrams of the received signals with 25, 50 and 100 GBd are shown in Fig. 3(b). The IQ-modulator has successfully achieved 100 GBd quadrature phase-shift keying (QPSK) modulation, resulting in a 200 Gbit/s data transmission with a BER of 3.64×10^{-3}. This value is under the threshold 4.5×10^{-3} for hard-decision FEC with a 7% overhead[13].

The fiber-to-fiber losses across several devices have been measured to be between 28 and 37 dB. From simulation results, we expect total insertion loss for the IQ-modulator in the order of 23.9 dB, of which 5.0 dB are attributed to the focusing grating couplers, 2.1 dB to the polarization rotator sections, 6.7 dB to the MIM phase modulators and the inherent 3 dB loss of IQ-modulator. Instead, in the experiment, we measured about 8 dB losses for the focusing grating couplers as derived from reference waveguides. The remaining excess losses can be attributed to non-ideal polarization rotators and MIM plasmonic phase modulators.

Conclusions

In conclusion, we introduced an all-metallic IQ-modulator and demonstrated data modulation with the QPSK format up to 100 GBd.

Acknowledgements

This work has been partially carried out at the Binnig and Rohrer Nanotechnology Center (BRNC). We acknowledge support from European Union grant 688166 PLASMOfab and European Research council grant 670478 PLASILOR.

References

[1] P. J. Winzer *et al.*, "From Scaling Disparities to Integrated Parallelism: A Decathlon for a Decade," *Journal of Lightwave Technology,* vol. **35**, no. 5, pp. 1099-1115 (2017).
[2] X. Zhou *et al.*, "Datacenter optics: requirements, technologies, and trends," *Chinese Optics Letters,* vol. **15**, no. 5, (2017).
[3] K. Schuh *et al.*, "Single carrier 1.2 Tbit/s transmission over 300 km with PM-64 QAM at 100 GBaud," in *Optical Fiber Communication Conference*, 2017.
[4] R. Going *et al.*, "Multi-channel InP-based Coherent PICs with Hybrid Integrated SiGe Electronics Operating up to 100 GBd, 32QAM," in *2017 European Conference on Optical Communication (ECOC)*, 2017.
[5] S. Wolf *et al.*, "Coherent modulation up to 100 GBd 16QAM using silicon-organic hybrid (SOH) devices," *Optics Express,* vol. **26**, no. 1, pp. 220-232 (2018).
[6] C. Haffner *et al.*, "All-plasmonic Mach-Zehnder modulator enabling optical high-speed communication at the microscale," *Nature Photonics,* vol. **9**, no. 8, pp. 525-528 (2015).
[7] C. Hoessbacher *et al.*, "Plasmonic modulator with > 170 GHz bandwidth demonstrated at 100 GBd NRZ," *Optics Express,* vol. **25**, no. 3, pp. 1762-1768 (2017).
[8] M. Ayata *et al.*, "High-speed plasmonic modulator in a single metal layer," *Science,* vol. **358**, no. 6363, pp. 630-632 (2017).
[9] B. Baeuerle *et al.*, "Driver-Less Sub 1 Vpp Operation of a Plasmonic-Organic Hybrid Modulator at 100 GBd NRZ," in *Optical Fiber Communication Conference*, San Diego, California, 2018.
[10] M. Burla *et al.*, "500 GHz plasmonic Mach-Zehnder modulator enabling sub-THz microwave photonics," *submitted for publication.*
[11] D. L. Elder *et al.*, "Effect of Rigid Bridge-Protection Units, Quadrupolar Interactions, and Blending in Organic Electro-Optic Chromophores," *Chemistry of Materials,* (2017).
[12] A. Josten *et al.*, "Modified Godard Timing Recovery for Non-Integer Oversampling Receivers," *Applied Sciences-Basel,* vol. **7**, no. 7, (2017).
[13] F. Chang *et al.*, "Forward Error Correction for 100 G Transport Networks," *IEEE Communications Magazine,* vol. **48**, no. 3, pp. S48-S55 (2010).